but been interpreted as homogeneous. For the parameter determination analysis, being omitted here because of lack of space, see Panneerselvam (2005). The local fitting results are also shown in Figs. 3 and 4 and are indicated as 'model' in the figures' captions. The tests performed by Sousa et al. (1993) are modeled as boundary value problems and solved for in ABAQUS®; cylindrical specimens were used with dimensions of 6 in diameter and 2 in height and the testing was kept within material's elastic range. In the first type of experiments the specimens were subjected to uniaxial compression under displacement control. The finite element results are compared to experimental results and this is shown in Fig. 3. The good agreement between experimental, FEM and local results is remarkable. In the second type of experiments a shear type of test is performed. A prescribed amount of horizontal displacement is applied at the upper surface of the cylinder whose height is kept constant throughout the test. The comparison between finite element, experimental and local results is shown in Fig. 4; as before, the agreement is remarkable.

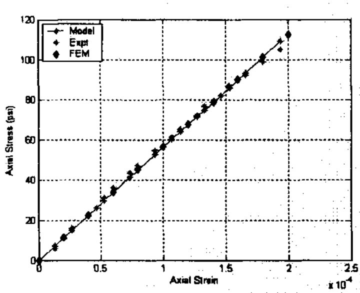

FIG. 3. Axial stress vs. axial strain. Comparison of finite element results to experimental data.

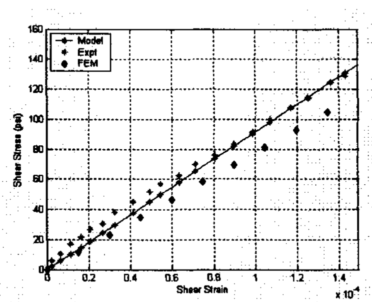

FIG. 4. Shear stress vs. shear strain. Comparison of finite element results to experimental data.

Hyperelastic-viscoplastic-damage model implementation in ABAQUS

The complete hyperelastic-viscoplastic-damage model is now implemented within the context of ABAQUS®. The implementation is carried out through user subroutine module UMAT. The algorithm described in the Box in conjunction to the consistent moduli given by Eqs. (18) and (19) are used. At each integration Gauss point UMAT is called for externally by the main program and stresses corresponding to strain states are obtained. The internal variables are updated at each time step through the user subroutine SDVINI.

The triaxial experiments performed by Tashman et al. (2004) and described earlier, are modeled as boundary value problems and solved for in ABAQUS®. The parameters which were obtained from the previous local simulation (in which the experiments were treated as being homogeneous, see Figs. 1 and 2) were used. The results from the finite element analysis are compared to the experimental data and this is shown in Fig. 5 and Fig. 6 for 0 and 15 psi confining pressure respectively.

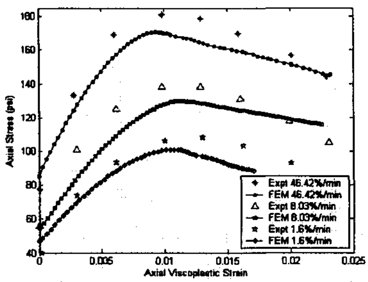

FIG. 5. Axial stress vs. axial viscoplastic strain. Comparison of finite element results to experimental data.

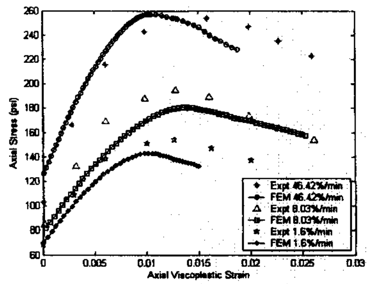

FIG. 6. Axial stress vs. axial viscoplastic strain. Comparison of finite element results to experimental data.

Next, the 'repeated simple shear test at constant height' (Sousa et al. 1993) is modeled as a boundary value problem. The RSST-CH experiment is conducted on the cylindrical specimens, which were described earlier in the monotonous experiments by Sousa et al. (1993), and the specimen is subjected to a repeated shear loading while the height of the specimen is kept constant. A haversine load of 0.05 s loading and 0.05 s unloading time is applied on a 0.2 in thick steel plate, which is glued to the cylindrical specimen. A remarkable characteristic of these experiments is that the accumulation of permanent shear strain with increasing number of cycles is a straight line on a log-log scale. The model is fitted to experimental results of 8 psi load amplitude and with the values obtained for the parameters the model's predictions to 10 psi loading amplitude are obtained. The results, which are shown in Fig. 7 are very good.

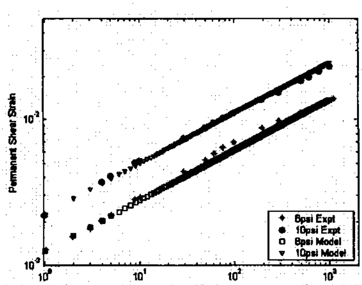

FIG. 7. Evolution of permanent shear strain with no. of cycles.

Finally, a section of a pavement, subjected to repeated tire pressure loading, is studied as a boundary value problem under plane strain conditions. This is a two dimensional model in which the two wheel pressure loads have been simulated as continuous loading strips, consistent with the plane strain assumption. The boundary conditions used in the model are consistent with physical conditions of the pavement and also the symmetry in the road section has been used effectively; this results in more efficient computational time. The asphalt concrete layer is taken to be 15 in deep and rests on a 40 in deep subgrade. The bottom edge and also the sides of the subgrade are fixed. The width of the half pavement is 80 in and the width of the subgrade is 160 in. The outer edge of asphalt pavement is assumed to be unsupported and is free to deform. Traffic load is applied as two tire pressure loads of magnitude 100 psi; the wheel loads are 10 in wide and they have a center to center distance equal to 12 in. The plane strain conditions, under which the complete model of the pavement section is studied, is a good assumption for a section of a highway where the traffic does not stop or start. A more complicated three dimensional pavement model could be used to represent pavement sections such as intersections, where traffic accelerates, decelerates or stands still. The asphalt concrete pavement is modeled using the hyperelastic-viscoplastic-damage model developed in this work. The subgrade is a granular material and a nonlinear material model would best represent its behavior. However, for simplicity and to keep the computational time shorter, the subgrade is modeled as a linear elastic material with elasticity modulus of 20000 psi and Poisson's ratio of 0.3; see Sousa et al. (1993). Figure 8 shows the deformed shape of the pavement at the end of 15 cycles, magnified 100 times, and also the stress distribution in the pavement section. The figure shows permanently deformed shape and also shows the upheavals to the sides due to shear flow and dilation and is similar to those observed in rutted pavement sections. This simulation of rutting pattern illustrates the capability of the model to study boundary value problems representing pavement sections as well as model's potential for rational analysis and design of pavements.

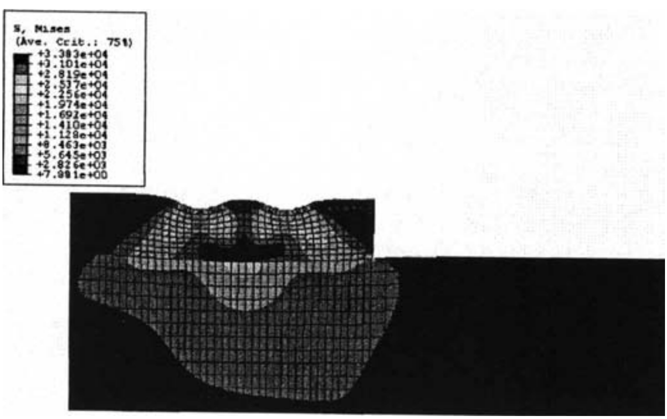

FIG. 8. Stress distribution in the deformed pavement.

ACKNOWLEDGEMENTS: The authors gratefully acknowledge financial support from the National Science Foundation, grant No. CMS-9802184.

REFERENCES

Panneerselvam, D., and Panoskaltsis, V.P., (2004) "Modeling and predicting the permanent deformations and damage of asphalt concrete: Analytical and computational aspects." Proceedings of the 17th ASCE Engineering Mechanics Conference, V. Kaliakin et al. eds., University of Delaware, Newark, Delaware, June 13-16. (Proceedings in CDROM form).

Panneerselvam, D., (2005) "Mechanics of Asphalt Concrete: Analytical and Computational Aspects", Ph.D. Dissertation, Department of Civil Engineering, Case Western Reserve University, Cleveland, Ohio.

Panoskaltsis, V.P. and Lubliner J. (1991), "Integration Algorithm for Frictional Materials Including Plasticity, Damage and Rate Effects", in *Anisotropy and Localization of Plastic Deformation*, J.-P. Boehler and A.S. Khan eds., Elsevier, London, pp. 651-654.

Simo, J.C., and Taylor, R.L., (1985) "Consistent Tangent Operators for Rate Independent Elastoplasticity," *Computer Methods in Applied Mechanics and Engineering*, **48**, 101-119.

Simo, J.C., and Hughes, T.J.R., (1998) Computational Inelasticity, Springer-Verlag, New York.

Sousa, J.B., Weissman, S.L., Sackman, J.L., and Monismith, C.L., (1993) "A Nonlinear Elastic Viscous with Damage Model to Predict Permanent Deformation of Asphalt Concrete Mixes", Transportation Research Record, 1384, 80- 93.

Tashman, L., Masad, E., Little, D., and Zbib, H. (2004), "Identification of Hot Mix Asphalt Permanent Deformation Parameters Using Triaxial Strength Tests and a Microstructure-Based Viscoplastic Continuum Model," Transportation Research Board, 83rd Annual Meeting, January 11-15, Washington, D.C.

THE HUET-SAYEGH MODEL; A SIMPLE AND EXCELLENT RHEOLOGICAL MODEL FOR MASTER CURVES OF ASPHALTIC MIXES

Adriaan C. Pronk[1]

ABSTRACT: The applicability of the Huet-Sayegh (H&S) model is shown for different asphalt mixes. The H&S model with only six parameters simulates in an excellent way the behavior of asphalt mixes in cycling tests over a very wide range of frequencies. Examples are given of these perfect fits for three completely different asphalt mixes. The only disadvantage is that the original model does not contain a viscous element for simulating the permanent deformation in contrast with the more familiar Burger's model. However, by adopting a linear dashpot in series with the H&S model an attractive alternative for the Burger's model is obtained which can be used over a large frequency range. Special attention is given to the mathematical operations connected to the use of the H&S model.

INTRODUCTION

Today the Burger's model is one of the traditional models for the characterization of the rheological behaviour of bituminous mixes. However, at a chosen temperature this model describes the response on a loading quite well but only for a limited range of frequencies. If the frequency for a sinusoidal load is varied over a large range the values for the elements in the Burger's model have to be changed. This disadvantage hampers the development of relationships between the model parameters and mix properties. Also there is a need for simple but good models in analytical and finite element programs. C. Huet (1965) has developed another model with the aid of so called parabolic dashpots, which is valid over a very wide range of frequencies (Pronk 2003a).

---

[1] Rijkswaterstaat Road and Hydraulic Engineering Institute, Ministry of Transport, Public Works and Water Management, P.O. Box 5044, 2600 GA Delft, The Netherlands, a.d.pronk@dww.rws.minvenw.nl

HUET-SAYEGH (H&S) MODEL

The Parabolic or Variable Dashpot

The characteristic rheological element in the H&S model is the parabolic or variable dashpot. The mathematical operation for the variable dashpot is only defined for sinusoidal signals as (Pronk 2003b):

$$\sigma\{e^{i\omega t}\} = \eta\tau^{a-1}\Omega^{a}\left[\varepsilon\{e^{i(\omega t-\varphi)}\}\right] = \frac{\eta}{\tau}.(i\omega\tau)^{a}\,\varepsilon\{e^{i(\omega t-\varphi)}\} \quad (1)$$

With $\sigma\{e^{i\omega t}\}$ is applied sinusoidal stress, $\varepsilon\{e^{i(\omega t-\varphi)}\}$ is the occurring sinusoidal strain, τ is a time decay constant, η is the viscosity and Ω is a special mathematical operator. Regarding Eq.1 the variable dashpot can be seen as a rheological element (for sinusoidal signals) between the linear spring (S.cos(φ); a = 0) and the linear dashpot (S.sin(φ); a = 1).

FIG 1. The response of a linear spring (X axis), a linear dashpot (Y axis), and a parabolic dashpot on a sinusoidal load.

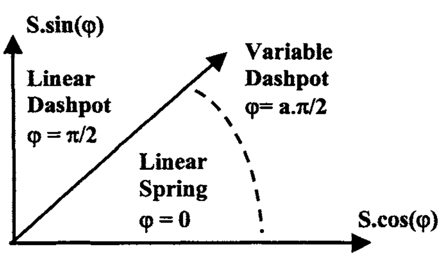

FIG 2. Scheme of the (general) H&S model

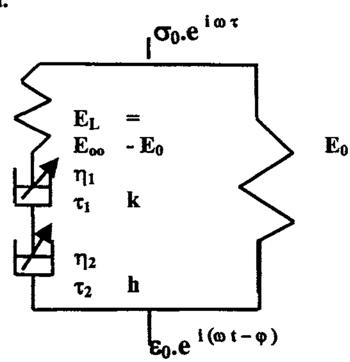

After a load the remaining deformation can be calculated with the aid of Eq. 2 (Pronk 1996) and will be zero for the variable dashpot if the parameter a is smaller than 1.

$$\varepsilon\{t \to +\infty\} = \underset{\omega \to 0}{Limit}\left[i\omega.\left\{\frac{1}{\eta.\tau^{a-1}.(i\omega)^{a}}\int_{-\infty}^{+\infty}\sigma.dt\right\}\right] = 0 \;\; for \;\; 0 < a < 1 \quad (2)$$

The general H&S model

The H&S model (figure 2) looks like a Zener model but instead of one linear dashpot (Zener model) it has two variable or parabolic dashpots. For sinusoidal signals ($e^{i\omega t}$) the response equation of a general H&S model will be (see also Annex):

$$S(\omega) = E_o + \frac{E_\infty - E_o}{1 + \delta_1 . (i\omega\tau_1)^{-k} + \delta_2 . (i\omega\tau_2)^{-h}} \tag{3}$$

with the following explanations:

$$\left.\begin{array}{c} S\{\omega\} = complex \quad stiffness \quad [MPa] \\ \omega = requency \quad [rad/s]; \tau_{1,2} = Time \quad constants \quad [s]; \\ \delta_{1,2} = \frac{\tau_{1,2}.(E_\infty - E_0)}{\eta_{1,2}} = Model \quad parameters \quad [-] \\ E_o = S\{\omega \to 0\} \ [Pa] \quad ; \quad E_\infty = S\{\omega \to \infty\} \ [Pa]; \\ 1 > h > k > 0 \quad ; \quad i = e^{+i.\frac{\pi}{2}} = cos\left(\frac{\pi}{2}\right) + i.sin\left(\frac{\pi}{2}\right) = 0 + i \end{array}\right\} \tag{4}$$

This general model has six parameters and two time constants but C. Huet (1965) decreased the number by taking only one time constant $\tau = \tau_1 = \tau_2$ (a "popular" explanation is given in Annex) and one constant $\delta = \delta_1$ ($\delta_2 \equiv 1$). The response $S\{\omega\}$ can be rewritten as:

$$S\{\omega\} = E_0 + \frac{E_\infty - E_0}{A^2 + B^2}.(A + B.i) \tag{5}$$

$$A = 1 + \delta . \frac{cos(k.\frac{\pi}{2})}{(\omega.\tau)^k} + \frac{cos(h.\frac{\pi}{2})}{(\omega.\tau)^h} ; B = 0 + \delta . \frac{sin(k.\frac{\pi}{2})}{(\omega.\tau)^k} + \frac{sin(h.\frac{\pi}{2})}{(\omega.\tau)^h} \tag{6}$$

Based on these formulas an Excel file has been made for a regression analysis. For this analysis four point-bending beam measurements (4PB tests) have been used at different frequencies and different temperatures. In contrast with the Burger's model the temperature influence can be included quite easily by adopting only a simple relation for the time decay constant τ.

$$\tau = e^{A_1 + B_1.T + C_1.T^2} \tag{7}$$

In most cases the coefficient C_1 can be taken equal to zero (see figure 3). In order to convergence to realistic values a restriction is needed for the static modulus E_0 ($E_0 \geq 0$

MPa; default 1 MPa is adopted as a seed value). Without this restriction and if the measured curve doesn't have data at low frequencies and/or high temperatures the regression analysis (the solver option in Excel) might lead unrealistic negative E_0 values.

APPLICATION OF THE H&S MODEL (EXAMPLES)

The stiffness measurements are carried out with the aid of four point bending tests in controlled strain mode. The applied strain amplitude was 50 mm/m. A maximum of 500 cycles were applied before the next higher frequency chosen. After the last frequency the first (lowest) frequency was applied again in order to check that no substantial fatigue damage has been induced. In the following figures the fitting is shown with the H&S model for three different asphaltic mixes. Based on an integrated regression analysis procedure the figures presented in table 1 were calculated for the three asphalt mixes (ZOAB, Güss Asphalt, and GAB).

TABLE 1. Results of the integrated regression analysis for the three mixes

						τ [s]		
Asphalt Mix	E_0 [MPa]	E_∞ [MPa]	h [-]	k [-]	δ [-]	A_1 [-]	B_1 [1/°C]	C_1 [1/°C]^2
ZOAB	150	18,000	0.224	0.656	0.082	-5.1	-0.28	0.0014
Güss Asphalt	10	34,400	0.173	0.456	0.25	-4.5	-0.35	0.003
GAB	1	37,400	0.144	0.558	0.037	-5.1	-0.39	0.003

FIG 3. Results of the (separate) regression for a Porous Asphalt (ZOAB) Cole-Cole diagram

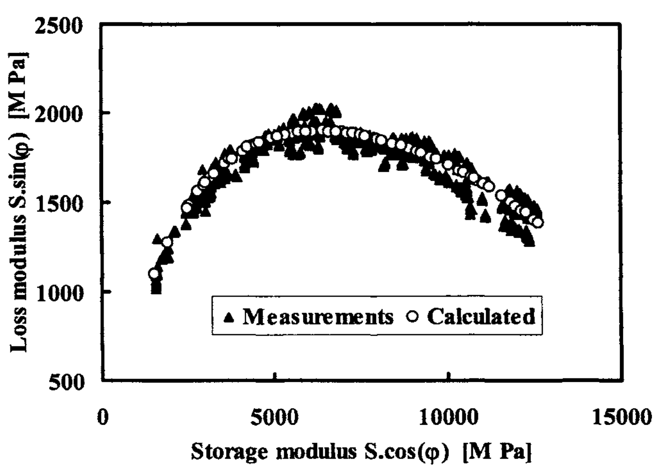

FIG 4. Results of the separate and integrated regression of τ as a function of temperature for a Porous Asphalt (ZOAB)

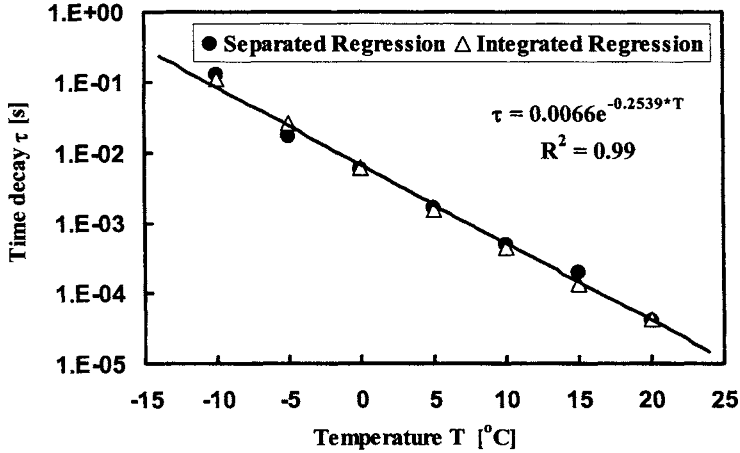

Porous Asphalt (ZOAB; very open graded mix)

This regression was carried out separately for all temperatures ranging from –10 to +20 °C. The frequency ranged from 5.9 to 58.6 Hz. At least 3 beams were tested. The complex stiffness modulus was measured between the 75th and 100th cycle. At that interval the target strain amplitude of 50 μm/m was always reached. The calculated time parameter τ is plotted in figure 4 as a function of the temperature. The same input data was also used for an integrated regression in which on forehand Eq. 7 was used for the τ dependency on the temperature. As clearly can be seen hardly no difference between these two regressions exists and that the regression coefficient C_1 in Eq. 7 can be omitted.

Güss Asphalt (penetration asphalt mix for dykes)

Güss Asphalt or in Dutch "Gietasfalt" is an asphalt mix used for (penetrating) sea dykes and steel bridges.. In figure 5 the frequency sweep measurements are given (at least three different beams were used per frequency; the frequency ranged from 5.9 to 58.6 Hz). The resulting master curves for stiffness and phase lag using the (integrated) H&S model are presented in figure 6. The stiffness and phase lag values are given as a function of the parameter $\omega.\tau$ with $\tau = A_1 + B_1.T + C_1.T^2$ with T in °C. The constants A_1, B_1 and C_1 follow from the integrated regression analysis.

FIG 5. Original frequency sweep data for a Güss Asphalt mix

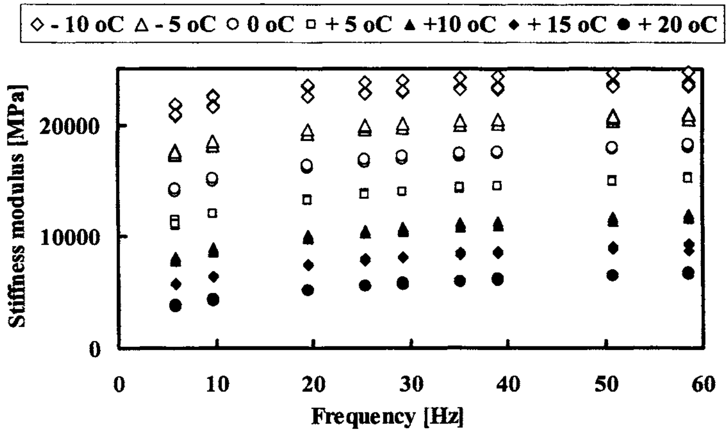

FIG 6. Master curves of the regression for a Güss Asphalt mix

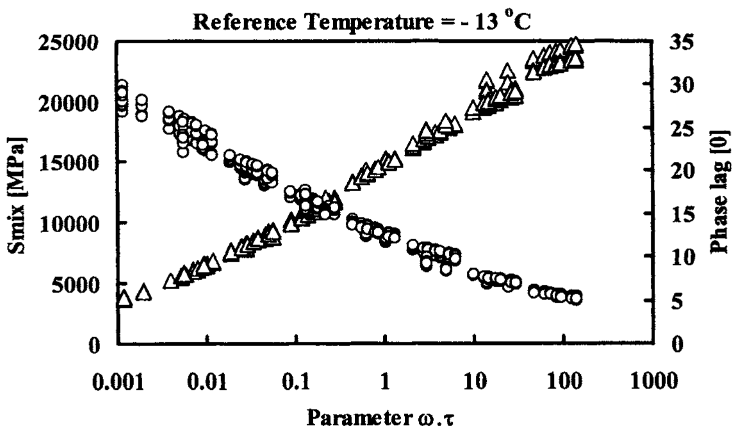

Gravel Asphalt Concrete (GAB)

This asphalt mix was used in trial sections of the LINTRACK (Montauban 1988). The stiffness modulus is measured in a four point bending test (4PB) in controlled strain mode. The values are taken at cycle 22. The frequency ranges from 2 to 29.3 Hz. Four beams were tested in the frequency sweep (see figure 8). The temperature was varied from –10 to +30 °C. A regression line of the form y = a.x is plotted in the figures for